Robot Pebbles: One Centimeter Modules for Programmable Matter through Self-Disassembly

Kyle Gilpin, Ara Knaian, and Daniela Rus

***Abstract*— This paper describes the design, fabrication, and experimental results of a programmable matter system capable of 2D shape formation through subtraction. The system is composed of autonomous 1cm modules which use custom-designed electropermanent magnets to bond, communicate, and share power with their neighbors. Given an initial block composed of many of these modules latched together in a regular crystalline structure, our system is able to form shapes by detaching the unnecessary modules. Many experiments show that the modules in our system are able to distribute data at 9600bps to their neighbors with a 98.5% success rate after four retries, and the connectors are able to support over 85 times the weight of a single module.**

I. Introduction

We present our newest programmable matter system, (see Figure 1), which is capable of forming shapes through self-disassembly. In general, programmable matter systems are composed of small, intelligent modules able to form a variety of macroscale objects in response to external commands or stimuli. Our system is composed of individual *pebbles* that are each approximately one cubic centimeter autonomous robots capable of bonding and communicating with their neighbors using custom electropermanent magnets. After starting from an initial configuration of modules, the system is able to self-disassemble to form complex 2D shapes. Each module in the system is able to communicate and latch with its neighbors using four novel electropermanent (EP) magnets. To date, we have built and tested five such smart pebbles, shown in Figure 1. Like a sculptor would remove the extra stone from a block of marble to reveal a statue, our system subtracts modules to form the goal structure.

A. System Functionality

We aim to create a system of sand grain sized modules that can form arbitrary structures with a variety of material properties on demand. Imagine a bag of these intelligent particles. If, for example, one needs a specific type or size of wrench, one communicates this to the bag. The modules contained within first crystallize into a regular structure and then self-disassemble in an organized fashion to form the requested object. One reaches in, grabs the tool, and uses it to accomplish a meaningful task. When one is done with the tool, it goes back into the bag where it disintegrates, and the particles can be reused to form the next tool. Such a system would be immensely useful for an astronaut on an inter-planetary mission or a scientist isolated at the South Pole. Even for the average mechanic or surgeon, the ability to form arbitrary, task-specific, tools would be immensely valuable in inspecting and working in tight spaces.

K. Gilpin, A. Knaian, and D. Rus are with the Computer Science and Artificial Intelligence Lab, MIT, Cambridge, MA, 02139, A. Knaian is also with the Center for Bits and Atoms at MIT. kwgilpin@csail.mit.edu, ara@mit.edu, rus@csail.mit.edu.

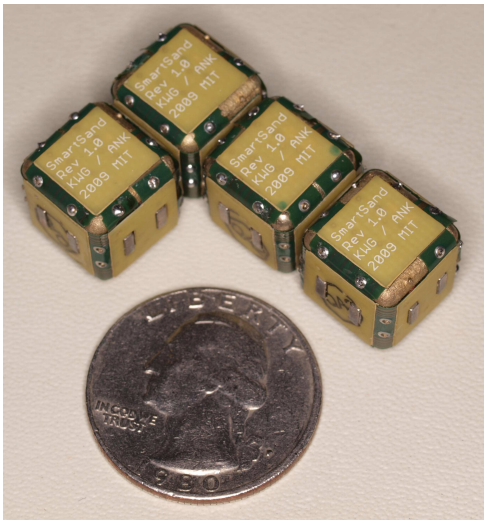

Fig. 1. Each programmable matter module is 12mm per side, and together they are able to form complex 2D shapes using electropermanent magnets able to hold 85 times the individual module weight.

B. Advantages of Self-Disassembly in the Pebbles System

Designing an electromagnetic module capable of exerting the force necessary to attract or repel other modules from a distance greater than the size of a module has proven challenging. Shape formation with electrostatic or magnetic modules is more feasible when driven by stochastic forces, so that the actuators only need to operate over short distances.

Program-driven stochastic self-assembly systems aim to form complex shapes in a single pass. The structure grows from a single module, surrounded by a sea of modules in stochastic motion. New modules are only allowed to attach to the structure at specific locations, and, over time, the desired structure grows in an organic manner. In contrast, our system aims to form complex shapes in two simpler passes. First, the modules form a crystalline block using self-assembly. Second, as shown in Figure 2, we complete the process by detaching the unwanted modules. External forces (e.g. gravity) then remove these modules from the structure.

Self-disassembly does not require precise alignment or careful planning, and does not expose delicate features of the finished object to high-energy stochastic motion, and

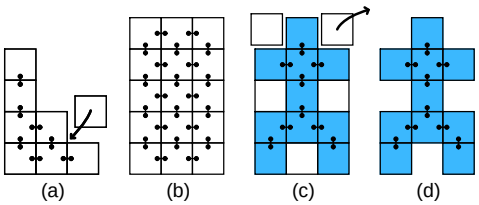

Fig. 2. To form shapes through subtraction, modules initially assembly into a regular block of material (a). Once this initial structure is complete and all modules are fully latched to their neighbors (b), the modules not needed in the final structure detach from the neighbors (c). Once, these extra modules are removed, we are left with the final shape (d).

thus is relatively quick and robust. Our modules are four-way rotation symmetric about a vector orthogonal to the assembly plane, and they can draw in and align with other modules over 2.4mm (20% module size) away. An inclined vibration table (in 2D) or a shaking bag (in 3D) should be sufficient to bring them into close enough proximity to enable the formation of a crystalline structure.

C. Related Work

Our research builds on previous work in programmable matter, self-assembly, and self-reconfiguring robotics. Several interesting program-driven stochastic self-assembly systems are under active development [1]–[3]. Like the robotic pebbles we propose, these systems rely on rigid particles for shape formation. While not able to reconfigure, the Digital Clay project [4] relies to particles able to bond using permanent magnets. Other approaches to shape formation rely on modules with internal degrees of freedom that are able to modify their topology in some way [5]–[7]. There are also hybrid systems [8]–[11] in which neighboring modules join to accomplish relative actuation.

Other research has focused more directly on the concept of programmable matter. One particular system [12], uses rigid cylindrical modules covered with electromagnets to achieve 2D shape formation. Theoretical research has previously investigated the use of sub-millimeter intelligent particles as 3D sensing and replication devices [13]. More recent developments are utilizing deformable modules [14] as a way to realize programmable matter. Finally, the system described in [15] has no actuation ability, but demonstrates what may be termed 'virtual' programmable matter through the use of 1000 distributed modules to form an intelligent paintable display capable of forming text and images.

A limited amount of past research has focused specifically on self-disassembling systems as a basis for shape formation [16]. This past work was based on large modules (45cm cubes) with internal moving parts. Additionally, the modules lacked symmetry so they had to be assembled in a particular orientation. The work presented in this paper is an outgrowth of the Miche system presented in [16], but we have reduced the module size, eliminated all moving parts, and added symmetry to allow for arbitrary module orientations. Finally, the system presented here shows promise as both a self-disassembling and self-assembling system.

II. Shape Formation by Subtraction

The system described in this paper represents a significant improvement on our previous Miche [16] self-disassembling shape formation system. The new pebble system uses smaller modules, operates without moving parts, does not depend on batteries, and uses EP magnets for latching, power transfer, and communication. We designed intelligent pebbles so that the algorithms used in the Miche will continue to function without modification. While the details of those algorithms are found in other works [16], we summarize them here to illustrate how the complete system functions.

Shape formation by subtraction proceeds through five basic stages: *neighbor discovery*; *localization*; *virtual sculpting*; *shape distribution*; and *disassembly*. In the first stage, *neighbor discovery*, modules are connected to form the initial structure. During this phase, modules detect when they are supplied with power and then attempt to communicate with and latch to their new neighbors. As the structure grows, modules keep track of with which neighbors they are able to communicate. After the initial structure has been assembled, the *localization* stage commences. All modules in the structure exchange local messages to determine their positions with respect to a root. All modules in the structure are able to to determine their relative coordinates without any concept of the structure as a whole. Each module then sends a reflection message containing its position back to the root. The root forwards these reflection messages to a GUI running on a PC, and the GUI builds a virtual model representing the initial arrangement of modules in the physical structure. Using this GUI model, the user drives the *virtual sculpting* stage by selecting which modules should be included in the final shape. After this sculpting process is complete, the program generates a sequence of inclusion messages. During the *shape distribution* stage, the GUI transmits these inclusion messages to a the root module. The structure then propagates these inclusion messages to their proper destinations. As with the localization process, the messages only contain local information. During the *disassembly* phase, the modules not designated to be in the final structure disconnect from their neighbors to reveal the shape the user sculpted previously. Each of the self-disassembly phases is dependent on a distributed, localized message passing algorithms executing on each module.

III. Hardware

Figure 1 shows four identical units of programmable matter. The modules are 12mm cubes capable of autonomously communicating with and latching to four neighboring cubes in the same plane to form 2D structures. Each completed module weighs 4.0g. The major functional components of each cube are power regulation circuitry, a microprocessor, and four EP magnets, which are responsible for latching, power transfer, and communication.

Each module is formed by wrapping the flexible circuit labeled (a) in Figure 3 around the brass frame labeled (b) that is investment casted around a 3D-printed positive model. The flex circuit is a two layer design, and the entire stack-up

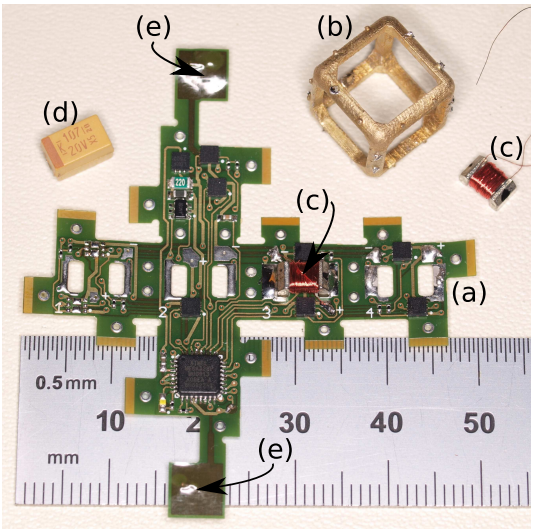

Fig. 3. Each module is composed of a flex circuit (a), a brass frame (b), four electropermanent magnets (c), and an energy storage capacitor (d) which mounts to the bottom of tabs labeled (e).

including solder masks is 0.127mm (5mils) thick. As seen in Figure 4, the flexible circuit is stiffened with 0.254mm (10mils) of Kapton in the six square areas corresponding to the six faces of the cube. The flex circuit is secured to the brass frame using a set of holes in the unstiffened portions of the flex circuit that mate with nubs on the frame. These holes and nubs align the flex circuit to the frame, and by soldering the flex circuit to the frame at these points, we form a secure bond between the circuit and the frame. This scheme allows for quick and easy disassembly of a module for service or debugging. Note, while a 3D system is theoretically possible, it would leave little room for electronics inside each cube. Additionally, the pole arrangement of the EP magnets would need to be made 8-way or axially symmetric.

A. Connection Mechanism

Figure 3 also shows two of the four custom designed EP magnets used in each module. These magnets are able to draw in other modules from a distance, mechanically hold modules together against outside forces (with zero power dissipation), communicate data between modules, and transport power from module to module. The EP magnets are soldered directly to the flex circuits so that their pole pieces protrude slightly through four sets of holes in the cube faces.

1) Electro-permanent Magnet Theory: As shown in Figure 4, each EP magnet consists of rods of two different types of permanent magnet materials, capped with soft-iron poles, and wrapped with a copper coil. One of the permanent magnets is Neodymium-Iron-Boron (NdFeB), and the other is Alnico V. Both of these materials have essentially the same remnant magnetization, about 1.2 Tesla, but very different coercivity; it takes about 100 times less applied magnetic field to switch the Alnico magnet than the neodymium magnet. A current pulse through the coil in the positive direction switches the polarization of the Alnico magnet so it is aligned with the polarization of the neodymium magnet. In this case, magnetic flux from both flows through the soft iron poles and to the other magnetic object, attracting it. The attraction continues after the current in the coil is returned to zero. We call this the "on" state of the connector. A current pulse through the coil in the negative direction switches the polarization of the Alnico magnet so it is opposite the polarization of the neodymium magnet. The polarization of the neodymium magnet is unchanged because it has a much larger coercivity. With the two magnets having opposite polarization, magnetic flux circulates inside the device but does not leave the poles, and thus does not exert force on the other connector or external ferromagnetic objects. Once again, this flux pattern continues after the current is returned to zero. We call this the "off" state of the connector.

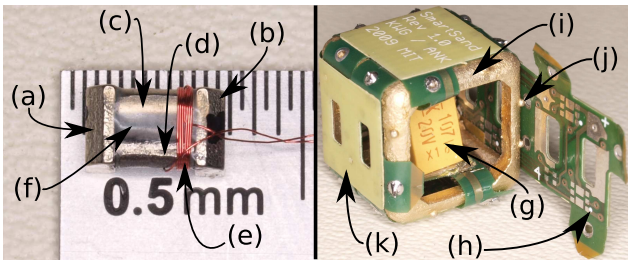

Fig. 4. Each electropermanent magnet assembly is composed of two pole pieces (a,b) which sandwich cylindrical Alnico (c) and NdFeB (d) magnets. The entire assembly is wrapped with 80 turns of #40 AWG wire (e) and held together using epoxy (f) (which makes the Alnico magnet appear larger than its NdFeB counterpart). The reservoir capacitors (g) used to energize the EP magnet coils are soldered to the flex circuit (h) which wraps attaches to the brass frame (i) with a set of nubs (j). Once mounted, the EP magnets protrude 0.25mm through the stiffener (k).

To understand the origin of bistability in an electropermanent magnet, it is helpful to examine the B/H (magnetic flux density vs. magnetic field intensity) plot shown in Figure 5. This is derived by adding the B/H plots for Alnico V and NdFeB, since the two magnets have the same area and same length, and appear in parallel in the magnetic circuit. Passing a current through the coil imposes a magnetic field, H, across the materials. The resulting magnetic flux density, B, passes through the air gap between the modules giving rise to an attractive force. While a positive current is flowing through the coil, it induces a positive magnetic field, H, saturating the Alnico magnet and driving the system to the point marked (a) in Figure 5. When that current is removed, the system relaxes back to a new equilibrium, labeled (b), with positive flux but no field. This is the "on" state. Momentarily passing a negative current through the coil saturates the Alnico magnet to the negative field side driving the system out to point (c) in Figure 5. Once the negative current is removed, the system relaxes to the zero field, zero flux "off" state marked by point (d). If the magnets are pulled apart while on, a demagnetizing field appears, reducing the flux and resultant force.

The electropermanent magnets used here are low average power but high peak power devices. Our system uses a 20V, 5A, 300μs pulse provided by a 100μF capacitor in each mod-

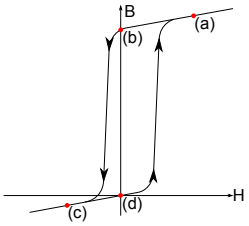

Fig. 5. The hysteresis curve for the EP magnet assembly shows the origin of the magnetic bistability in the device.

ule to switch their state. The time-averaged power devoted to magnetic attraction is many orders of magnitude lower than would be required using equivalent electromagnets. We calculate that an equivalent electromagnet would consume 10W continuously. The EP magnet consumes 100W over 300μs when switching (on or off). Therefore, so long as the EP magnet is switched less than once every 3ms, the EP magnet will use lower time-averaged power. For more information about the EP magnets, including detailed design guidelines and a quantitative model, see [17], [18].

2) Electropermanent (EP) Magnet Construction: The magnetic rods and pole pieces were custom fabricated by BJA Magnetics Inc. The magnetic rods are grade N40SH NdFeB, and cast Alnico 5, both 1.587mm diameter and 3.175mm long, magnetized axially. The magnetic rods were fabricated by cylindrical grinding. The magnetic rods were coated with 5μm of Parylene by the Vitek Research Corporation. The pole pieces are 3.175mm by 2.54mm by 1.27mm blocks of grade ASTM-A848 soft magnetic iron, with a diagonal notch cut off to allow clearance when four are placed inside the cube. The pole pieces were fabricated by wire EDM, and chromate coated to slow corrosion and facilitate solderability. The rods and pole pieces were assembled with tweezers under magnification, using a mounting plate with slots to hold the pole pieces and a center support to hole the magnetic rods. The rods are glued to the pole pieces using Loctite Hysol E-60HP 60-minute work time epoxy (Henkel Corporation). After assembly, the pole faces are flattened by rubbing the assembly against a 320 grit aluminum-oxide oil-filled abrasive file (McMaster-Carr). An 80-turn coil is wound around the magnetic rods using #40 AWG magnet wire (MWS Wire Industries).

3) Power Electronics: The four electro-permanent magnets in each cube are driven by a set of 2mm square MOSFETs which are capable of handling the 5A required to switch the EP magnets (Fairchild Semiconductor FDMA2002NZ and FDMA1027P). In order to reduce the component count, we avoided driving each EP magnet coil with its own full H-bridge. Instead, each EP magnet has one dedicated half-bridge connected to one side of its coil. We call these the "face-specific" drivers. The other sides of the four coils are tied together and serviced by a single "common" half-bridge as shown in Figure 6. Using this configuration, we are able to pass current in both directions through each of the EP magnet coils, one coil at a time.

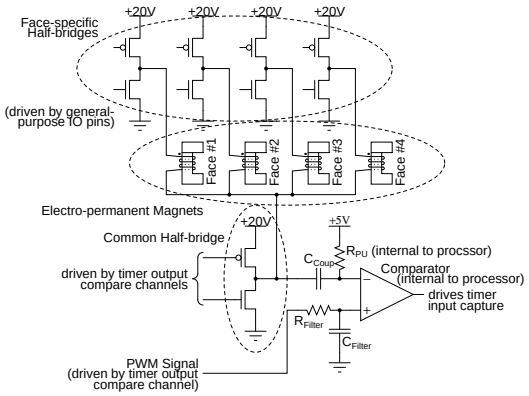

Fig. 6. The four EP magnets are driven by a set of four face-specific half-bridges and one common half-bridge in order to reduce the modules' component count and circuit area. C_{Coup} allows the processor to detect communication pulses from neighboring modules. Except for four level shifters used to drive the PMOS devices, a voltage regulator, LED, and the processor, this is essentially the entirety of the electronics in each module.

B. Processors

Each module is controlled by an Atmel ATmega328 processor which offers 32KB of program memory and 2KB of RAM in a 5mm square package. To minimize the external component count, we employ the processor's internal 8MHz RC oscillator as the processor's primary clock source. We routed the processor's SPI and debugWire pins to pads on the outside of each cube. We constructed a test fixture to contact these pads to allow us to communicate with, program, and debug the modules.

C. Communication Interface

The EP magnets form an inductive communication channel between neighboring modules. In short, when two EP magnets are in contact, they behave just like a 1:1 isolation transformer. We utilize this fact to transfer data between modules without affecting their ability to latch together. All inter-cube communication occurs at 9600bps using a series of 1μs magnetic pulses induced by the coil of one EP magnet and sensed by the coil of the neighboring EP magnet assembly. The presence of a single 1μs pulse during a bit period signifies a logical '1' while the lack of any pulse signals a '0'. Neighboring modules transfer data using pulses of the same polarity as the pulses used to latch the EP magnets. As a result, there is no risk of the latching strength decreasing over time during intensive communication.

Because the four EP magnets share a common half-bridge, a module is unable to discriminate between incoming messages if it is listening for messages on multiple faces. To select the face on which the cube is listening, the face-specific high-side MOSFET of one face is turned on while the three others coils are left floating. Additionally, the common side of all four EP magnet coils is left floating, but it is capacitively coupled by C_{Coup} to the processor's analog input. The internal pull-resistor (R_{PU}) on this analog input is enabled. Internally, the processor routes this signal to the

inverting input of the its internal analog comparator. Figure 6 shows the components used when receiving a message.

The non-inverting input of the processor's comparator is driven by a DC voltage that we generate by low-pass filtering the output of another of the processor's timer channels. Specifically, we employ one of the processor's output compare channels to generate a variable duty cycle square wave. As shown in Figure 6, this square wave is filtered by a passive first-order RC filter (R_{Filter} and C_{Filter}) to produce DC level which varies with duty cycle.

The cube sending data to a neighbor does so by applying a $+20V$ pulse between the face-specific side and the common side of one of its EP magnet coils. This will induce a negative-going voltage spike on the C_{Coup} capacitor in the neighboring cube. When these spikes drop below the threshold voltage of the comparator, it's output will transition from low to high to signaling a bit.

D. Power

The modules in our programmable matter system do not contain their own power sources. Instead, electrical power is distributed from one or more centralized sources and then transferred from one cube to the next. Power is transferred between units via Ohmic conduction of DC power through the soft magnetic poles of the connectors. Each module contributes a resistance of 0.3Ω. Given that the quiescent current of each module is 15mA, each module in a chain results in a voltage drop of 4.5mV. In theory, a 20V source could power a chain of 3266 modules before the voltage supplied to the trailing module falls below the dropout voltage of the regulator used to power the microprocessor. In practice, the ability of the electropermanent magnets to change state would be compromised much sooner. Additionally, any real system consisting of more than a chain of modules would provide many parallel electrical paths that would noticeably reduce the electrical resistance between any two points.

Within each cube, the EP magnets are mounted to the flex circuit, which serves as an elastic mount, allowing slight bending as needed for the two magnetic connectors to achieve intimate contact. When one magnet is turned on, it attracts any nearby neighbor; contact is achieved; the adjacent cube receives power, starts its program; and the two cubes communicate to drive a series of synchronized pulses through their magnets to bond more strongly. All of the magnetic materials used in the connector are good conductors of electricity, so it was necessary to coat the rods of Alnico and NdFeB separating the two poles with Parylene to electrically isolate the two poles.

Each module contains a 100μF low equivalent series resistance, (low ESR), reservoir capacitor. These capacitors, one of which is labeled (d) in Figure 3, are responsible for sourcing the high-current demands of the EP magnets when they are switching on or off. These capacitors fill the interior of each cube and can only be installed once the flex circuit is partially folded around the brass frame. Instead of being mounted as a traditional surface mount capacitor would, the storage capacitor is soldered by its ends to the bottoms of two tabs labeled (e) in Figure 3.

The connectors on the four mating sides of the cube are identical, and placed so that the magnetic North is always on the right (when viewing the face head-on), and the magnetic South is always on the left. Regardless of their rotations about a vector orthogonal to the assembly plane, when two cubes are placed together, the magnets will align North-to-South. Internal to each cube, all of the North poles of the EP magnets are tied together in one net, and all of the South poles are connected in another. Therefore, in a chain of modules, the North pole net will alternate between serving as the electrical ground and the 20V rail. In a large network of cubes, every circular path back to the same cube passes through an even number of connector pairs, so there is no arrangement than can result in a short circuit. Internally, a bridge rectifier is used produce a voltage with known polarity from the unknown polarity present on the North and South pole nets. As a result, the cubes are four-way rotation symmetric.

By using a capacitor instead of a battery for energy storage in the module, we are able to decrease their size and complexity. Compared with capacitors, batteries are larger, more toxic, shorter-lived, and require additional charging and protection circuitry. If, during the course of additional development, we find that the system must be untethered from all power sources, we envision creating and deploying a limited number of passive battery modules to be mixed with the active modules described here.

IV. Control Algorithms

We have implemented several low-level algorithms on the modules' processors which drive the latching and communication processes. These algorithms provide an abstraction barrier and a useful API for higher level algorithms. The current latching and communication algorithms consume 11.7% of the processor's program memory leaving close to 29KB for high-level shape formation algorithms.

A. Communication

Because the hardware prevents a module from listening for incoming messages on multiple faces simultaneously, the software divides its time listening for incoming messages between a module's four faces. If the processor does not detect an incoming messages on a face for 25ms, it proceeds to listen on the next face. The impacts of this scheme are discussed in the Experiments section below.

In addition to rotating through all faces, the software also ensures successful communication by employing bidirectional handshaking before any data is transferred between neighboring modules. This handshaking is necessary for two reasons. First, because each module is driven by an RC oscillator, non-trivial differences in clock frequency make asynchronous communication challenging. Second, we need a way to ensure that as a receiver selects a new face on which to listen, it is able to correctly detect the start of the neighboring transmitter's data. We accomplish both these

objectives by employing two unique synchronization bytes at the start of each exchange. The transmitter first sends a synchronization byte consisting of all ones. The receiver, if it is listening, uses the spacing between the received synchronization bits to adjust its bit timing before echoing the synchronization byte. Only after the transmitter detects this echoed byte does it proceed to send data.

B. Latching

The algorithms which control the latching and unlatching of neighboring modules are built on the inter-cube communication algorithms. While neighboring modules are able to activate and deactivate their EP magnets independent of each other, synchronized latching produces the highest holding force. A module initiates a synchronized latch operation using the inter-module message passing procedure described above. The content of the message exchanged is a single character that does not appear in any other type of message. Once this character is exchanged between modules, the receiver waits 160μs, the transmitter finishes sending several stop bits, and then both modules energize their respective EP magnet coils within 1μs of each other. To ensure the strongest possible bond between neighbors, the modules can repeat this procedure multiple times. The unlatching process is identical to the latching process. The module which wishes to separate from the larger structure uses the same handshake based communication protocol to send another unique character to all of its neighbors. Shortly after this character is received, both modules pulse their EP magnet coils to release their hold on one another.

V. Experiments

In order to prove that the hardware and software described above operates correctly, we performed over 60 tests of the EP magnets' strength and exchanged over 30,000 inter-module messages. To demonstrate that the inter-module power transfer system was functional, all of these experiments were performed while the modules were relaying power from one module to the next.

A. Communication

In previous work [16], inter-module communication proved to be a major bottleneck to overall system performance. To ensure that our system is scalable, we tested both how quickly and how reliably a group of modules was able to communicate. In each case, we ran a series of four related experiments. In each experiment, one, two, three, or four transmitting modules were mated to a central receiving module. Each transmitting module attempted to send a string of messages consisting of increasing numbers: "1", "2", "3", etc. The transmitting modules were attempting send these messages on all of their faces (i.e. "3" was transmitted from all faces before attempting to do the same with "4"). If the receiving cube did not respond to a transmitting module's attempt to transmit, the transmitting module progressed to the next number. The receiving cube was connected to a power source and also shared a serial communication link with a desktop PC running a terminal program. The receiving cube's only task was to listen for incoming messages on each of its four faces and relay these messages to the desktop computer. able I summarizes the results of our communication speed test. In each case, we measured how many messages were received in the first 60 seconds after all cubes were energized.

TABLE I

The inter-module message exchange rate is roughly linearly related to the number of neighboring modules transmitting messages.

# Transmitters	*Rate [msg/sec]*	*Rate per Face [msg/sec]*
1	10.4	10.4
2	20.5	10.3
3	39.3	13.1
4	50.9	12.7

The communication speed test shows that the message reception rate is, in the worst case, 10 messages per second, but grows in proportion to the number of transmitters. This is not surprising given that the receiver listens for incoming messages on each face for a set amount of time before proceeding to listen on the next face. In the event that the receiver does receive a message while listening to a specific face, it immediately advances to listening on the next face. In the experiments summarized in Table I, the receiver was programmed to linger and listen on each face for 25ms, but the messages being transmitted were roughly half this length. (Given our experience with the Miche system [16], we expect the average message employed the the disassembly algorithms to be 15 characters in length and therefore require 12.5ms to transmit.) If the receiver receives a message each time it listens to each face, it will be able to progress through its tour of all four faces more quickly. This explains why the per-face message reception rate was greatest when the receiver had three of four neighbors.

To test how reliably neighboring cubes were able to communicate, we performed two experiments. The first was designed to test the reliability of the communication channel; the receiver listened for incoming messages on only one face. We allowed the single transmitter to send over 10,000 messages, but not a single message was lost or received incorrectly. The inter-module communication channel is quite robust. In the second experiment, the receiver divided its time by listening for incoming messages on all four faces. We measured both the fraction of messages received as well as the number of attempts each transmitting cube made before it was successful. Table II shows what percentage of transmitted messages were received and passed to the PC.

The results for the second experiment show that as the number transmitters is increased, the percentage of messages that are received also increases. This trend is due to the phenomenon described above: the receiving cube is able to cycle through listening for incoming messages on all faces more quickly when it is actually receiving messages on all faces. (It should be noted that this result will only hold when the received messages require less time to transmit

TABLE II

THE PERCENTAGE OF MESSAGES RECEIVED BY A MODULE WITH MULTIPLE TRANSMITTING NEIGHBORS INCREASES WITH THE NUMBER OF NEIGHBORS.

# Transmitters	*% Messages Received*
1	25.0
2	25.0
3	26.4
4	30.2

than the time spent by the receiving cube dwelling on each face.) While not shown here, we examined the distribution of dropped messages. We found that for any number of transmitting neighbors, the percentage of the time a transmitter unsuccessfully attempted to communicate with the receiver before success was rarely more than three attempts. If the transmitters were programmed to retry sending each message until successful, a transmitter would, on average, succeed within 4 attempts 98.5% of the time. As shown by the first reliability experiment, the failures in the other 1.5% of cases are not due to a noisy channel but the fact that the receiver was never listening while the transmitter was active.

B. Latching

To test the strength of the magnetic connectors and to compare the efficacy of different drive waveforms, we performed pull tests using two cubes. One cube was mounted on a linear motion stage, the other on an air bearing, with a load cell measuring the force along the air bearing's allowed direction of motion. (For details about this experimental setup, see [17]. For each of the pull tests, the module attached to the motion stage is connected to an external power source through an attached magnetic connector. The linear stage is used to bring the modules together. When they come into contact, the second cube powers up, and the two exchange synchronization message.

The normal force resulting from three different latching waveforms is shown in Figure 7. The average holding force, (over nine tests), for two asynchronous pulses, (one from each magnet), was 2.16N. When both magnets were pulsed synchronously, the resulting force was 2.06N (averaged over 15 tests). When both magnets were pulsed synchronously twice, the average peak force was 3.18N (averaged over 4 tests). These results make physical sense. Synchronous pulses produce a stronger magnetic field, and repeated application of this field drives the EP magnet farther into the first quadrant along its B-H curve resulting in a larger remnant flux. In addition to the normal force required to separate two cubes, we measured the shear force between two cubes using the same fixture. It was difficult to separate the effects of friction from the shear magnetic force. Five shear tests yielded forces of 0.22–0.83N with an average of 0.69N. Finally, we measured the remnant normal force after the magnets had been switched off to determine whether unused modules in a larger structure would easily separate from the goal shape. In ten trials, we were unable to measure any remnant force holding the modules together after their EP magnets had been deactivated. (The measurement noise of the force sensor is zero-mean with a standard deviation of 0.0068N.) We can use the fact that a magnetically suspended EP magnet naturally falls off of its mating surface when deactivated to upper-bound the remnant force by 0.002N (the force due to gravity on a single EP magnet).

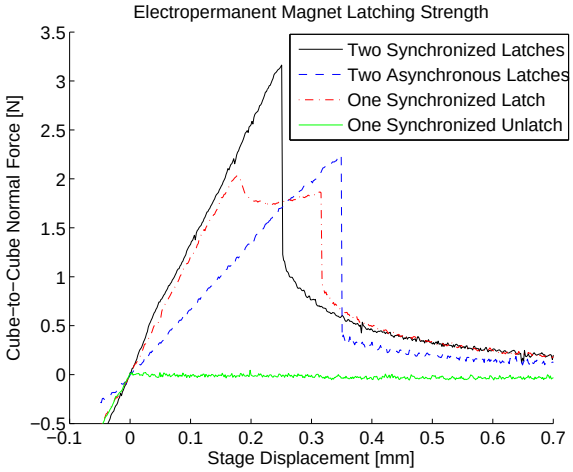

Fig. 7. The latching force between cubes is strongest when each cube energizes its magnet assembly with two synchronized latching pulses space far enough apart that the 100μF reservoir capacitors have time to recharge.

All three traces show an initial linear rise in force with displacement, corresponding to the elastic deformation of the cubes, (and the load cell spring), in the fixture as they are pulled apart before the magnetic connectors separate. A peak is reached, and then the LED in the load-cell-side cube extinguishes, corresponding to separation of at least one pole of the connectors, and the force decreases as the air gap distance between the magnets increases.

The distance over which the connectors remain in contact as the stage displacement increases, (the distance from 0 displacement until the peak force), provides a way to measure the tolerance to nonuniformity and misalignment in a large collection of modules. A large network of cubes is mechanically over-constrained, so one might be concerned about the ability to get reliable power transmission between modules, which requires continuous contact. From the pull tests, one can see that a displacement between 0.25–0.35mm (2–3% of the total module size) is possible before separation, allowing a large network of cubes to achieve precision connector alignment through elastic averaging.

Figure 8 illustrates the coil current and voltage during a single synchronized pulse. Looking at the voltage and current data, we can see that the current reaches a momentary peak and then decreases during the pulse, indicating that the magnetic material is not saturating during the pulse, but that the peak current is instead limited by the discharge of the capacitor. This was the inspiration for the double synchronous pulse, (which energizes the coils a second time after waiting for the capacitor to recharge), and as Figure 7 shows, it does reach a higher force level. The force measured

for the double synchronous pulse is 72% of the 4.4N figure measured in [17] for a single magnet being pulled away from an iron plate, in which a stiff power supply was used and full saturation of the magnetic material achieved.

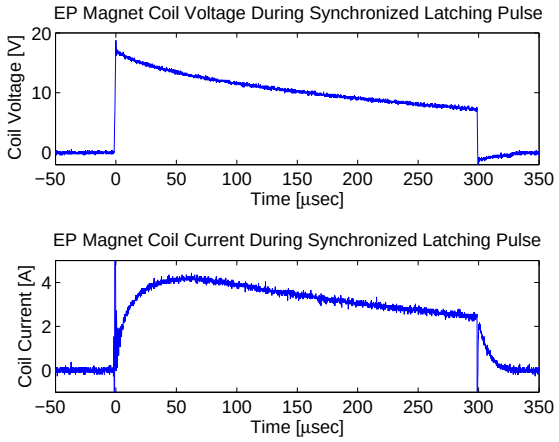

Fig. 8. The EP magnet coil current peaks and then falls during a 300μs latching pulse indicating that the magnets are not fully saturated. The current does not reach a plateau because the capacitor discharges too quickly. (Ignore the short switching transients in the current data.)

In addition to testing the modules' ability to remain connected, we wanted to verify their ability to draw in and latch with other modules in close proximity. We performed two different experiments. In the first, one module had its magnets off while the other module had its magnets on. One module was fixed while the other was free to move on the non-sticky side of cellophane tape. The modules were aligned and their faces parallel. In 30 trials, the modules always successfully attracted and latched when their initial separation was 2.48mm. The second experiment was identical except that the magnets in both modules were energized. In 28 of 30 trials, the two modules latched from an initial separation of 4.31mm. These experiments encourage the idea that a collection of modules will be able to successfully self-assemble in the presence of stochastic environmental forces.

VI. Discussion

Our experiments show that the hardware and low-level software of our robotic pebbles are a viable basis for a programmable matter system. The EP magnets proved effective transferring power, binding modules together, and exchanging data. Future work will have several focuses: producing more modules; implementing higher-level algorithms; extending the system to 3D by exploring alternate magnet and module geometries; and shrinking the individual module size. While our system has not yet reached true sand-sized proportions, the modules presented here are among the smallest modules for self-assembly or self-disassembly of which we are aware. Furthermore, the system has no moving parts and does not require batteries. These are both critical requirements for any system that could eventually be produced en masse by an integrated semiconductor process. With continued research, we are hopeful that this can become a reality within the not too distant future.

VII. Acknowledgments

This work is supported by the DARPA Programmable Matter program (Dr. Mitch Zakin, PM) and the US Army Research Office under grant numbers W911NF-08-1-0228 & W911NF-08-1-0254, NSF EFRI, MIT Center for Bits and Atoms, Intel, and the NDSEG fellowship program. We thank Profs. Rob Wood, Neil Gershenfeld, Joe Jacobson, Sangbae Kim, and their students, especially Sangok Seok, Sam Wald, and Krishna Settaluri.

References

[1] P. White, V. Zykov, J. Bongard, and H. Lipson, "Three dimensional stochastic reconfiguration of modular robots," in *Robotics Science and Systems*. MIT, June 8-10 2005.

[2] M. Tolley, J. Hiller, and H. Lipson, "Evolutionary design and assembly planning for stochastic modular robots," in *IEEE Conference on Intelligent Robotics and Systems (IROS)*, October 2009, pp. 73–78.

[3] S. Griffith, D. Goldwater, and J. M. Jacobson, "Robotics: Self-replication from random parts," *Nature*, vol. 437, p. 636, September 28 2005.

[4] M. Yim and S. Homans, "Digital clay," WebSite. [Online]. Available: www2.parc.com/spl/projects/modrobots/lattice/digitalclay/index.html

[5] M. Yim, Y. Zhang, K. Roufas, D. Duff, and C. Eldershaw, "Connecting and disconnecting for self–reconfiguration with polybot," in *IEEE/ASME Transaction on Mechatronics, special issue on Information Technology in Mechatronics*, 2003.

[6] A. Castano, A. Behar, and P. Will, "The conro modules for reconfigurable robots," *IEEE Transactions on Mechatronics*, vol. 7, no. 4, pp. 403–409, December 2002.

[7] A. Kamimura, H. Kurokawa, E. Yoshida, S. Murata, K. Tomita, and S. Kokaji, "Automatic locomotion design and experiments for a modular robotic system," *IEEE/ASME Transactions on Mechatronics*, vol. 10, no. 3, pp. 314–325, June 2005.

[8] M. E. Karagozler, S. C. Goldstein, and J. R. Reid, "Stress-driven mems assembly + electrostatic forces = 1mm diameter robot," in *IEEE Conference on Intelligent Robots and Systems (IROS)*, October 2009, pp. 2763–2769.

[9] E. Yoshida, S. Murata, S. Kokaji, A. Kamimura, K. Tomita, and H. Kurokawa, "Get back in shape! a hardware prototype self-reconfigurable modular microrobot that uses shape memory alloy," *IEEE Robotics and Automation Magazine*, vol. 9, no. 4, pp. 54–60, 2002.

[10] M. Koseki, K. Minami, and N. Inou, "Cellular robots forming a mechanical structure (evaluation of structural formation and hardware design of "chobie ii")," in *Proceedings of 7th International Symposium on Distributed Autonomous Robotic Systems (DARS04)*, June 2004, pp. 131–140.

[11] G. Chirikjian, A. Pamecha, and I. Ebert-Uphoff, "Evaluating efficiency of self-reconfiguration in a class of modular robots," *Journal of Robotic Systems*, vol. 13, no. 5, pp. 317–388, 1996.

[12] S. Goldstein, J. Campbell, and T. Mowry, "Programmable matter," *IEEE Computer*, vol. 38, no. 6, pp. 99–101, 2005.

[13] P. Pillai, J. Campbell, G. Kedia, S. Moudgal, and K. Sheth, "A 3d fax machine based on claytronics," in *International Conference on Intelligent Robots and Systems (IROS)*, October 2006, pp. 4728–4735.

[14] J. John Amend and H. Lipson, "Shape-shifting materials for programmable structures," in *International Conference on Ubiquitous Computing: Workshop on Architectural Robotics*, September 2009.

[15] W. Butera, "Text display and graphics control on a paintable computer," in *Conference on Self-Adaptive and Self-Organizing Systems (SASO)*, July 2007, pp. 45–54.

[16] K. Gilpin, K. Kotay, D. Rus, and I. Vasilescu, "Miche: Modular shape formation by self-disassembly," *International Journal of Robotics Research*, vol. 27, pp. 345–372, 2008.

[17] A. Knaian, N. Gershenfeld, and D. Rus, "Switchable electropermanent magnets: Design, modeling, and fabrication," *In preparation*, 2010.

[18] D. F. Pignataro, "Electrically switchable magnet system," U.S. Patent 6,229,422, 2001.